Chalmers Publication Library

Copyright Notice IET

(Article begins on next page)

High/Low Impedance Transmission Line and Coupled Line Filter Networks for Differential Phase Shifters

Peter Sobis, Jan Stake and Anders Emrich

Abstract—**Two compact and simple to design differential phase shifter topologies, based on high/low impedance transmission line sections and open-ended coupled line sections, are presented for the first time. The basic circuit theory for single section topologies is reviewed, leading to design equations and graphs for direct circuit synthesis. Balanced topologies and multiple section designs are also proposed improving the performance and feasibility of the phase shifters. Two planar microstrip single section differential phase shifter hybrids, at a centre frequency of 12 GHz and a 45° and 135° phase difference have been designed and manufactured. The designs have a simulated 0.5 dB amplitude and 1° phase imbalance over more than 25% and 40% bandwidth, respectively. Experimental results verify the circuit performance and feasibility of the proposed differential phase shifters.**

Index Terms— **Microwave Phase Shifters, Differential Phase Shifters, Power dividers.**

I. Introduction

Differential phase shifters have a wide area of applications in the microwave field ranging from antenna beamforming networks such as Butler-matrices [1] and digital phase shifters [2] to various feed networks for balanced amplifiers, multipliers and mixers [3]-[6]. In contrast to variable phase shifters that offer

active control of the phase response, which can be used for designing steerable antenna arrays and tunable delay lines, etc., differential phase shifters are used in applications requiring a fixed through phase difference between electrical paths. A comparison between different topologies is given in table 1, in [7] a general introduction to phase shifters can be found. At lower frequencies differential phase shifters can be synthesised using LC-networks [8]; at higher frequencies, mainly due to parasitic effects, distributed components and transmission-line type networks are typically used. By loading an uncoupled pair of lines of different lengths with a dispersive element such as a bandpass filter, an almost constant phase difference between S_{21} and S_{43} can be achieved over a considerable bandwidth, see Fig. 1. Two common transmission line based bandpass structures that are used in differential phase shifters are stub-loaded lines [9] and coupled line Schiffman sections [10]-[11].

However, both types of structures depend on circuit elements with a lateral distribution; this could constrain the overall circuit layout or in some cases not be implemented due to space limitations.

In [12] Wilds introduces an alternative circuit structure with minor lateral extension combining stub-loading, open-ended coupled lines and high to low impedance transitions, with a similar performance as Schiffman type phase shifters. The main advantages of this topology is the reduced width of the filter element and that the structure itself can be simultaneously utilised for signal distribution, two desirable properties in applications requiring tightly packed circuitry with little or no available space in the lateral direction.

In this paper, based on a theoretical analysis, it is shown for the first time how high/low impedance half wavelength long transmission line sections and homogenous open-ended coupled-line filters [13] respectively, can be utilised for designing simple and compact differential phase shifters with in some cases up to octave bandwidths. As only one type of filter structure is used, and not three compared to [12], the circuit design is simplified considerably. Design equations and graphs for direct circuit synthesis are presented together with the experimental results of the proposed differential phase shifter topologies.

II. Theoretical Analysis and Simulations

The following analysis begins by stating the ABCD parameters of the individual filter circuit elements. The ABCD parameters are subsequently transformed to S-parameters leading to explicit equations of the through phase characteristics as a function of the circuit parameters. A typical phase response of a differential phase shifter is shown in Fig. 2, from which the relative bandwidth B is calculated as:

$$B = \frac{\theta_{high} - \theta_{low}}{\theta_0}$$

(1)

with a phase ripple R equal to:

$$R = \Delta\varphi_{max} - \Delta\varphi_0 = \Delta\varphi_0 - \Delta\varphi_{min}$$

(2)

The analysis continues by calculating the phase imbalance and bandwidth analytically or numerically, this is done by using a matched condition at the centre frequency leading to graphs for direct circuit synthesis.

TABLE I
QUALITATIVE COMPARISON OF VARIOUS DIFFERENTIAL PHASE SHIFTER TOPOLOGIES

TYPE	CHARACTERISTICS	APPLICATIONS	REFERENCES
Single/Balanced Schiffman Multisection Schiffman	Coupled lines λ/4 long Tapered	Broadband, high performance, planar circuits Ultrawideband 10:1	[10],[14],[15]
Stub Loading	Open/shorted parallel stubs, λ/4 apart, simple structure	Narrowband, planar circuits and waveguides	[9]
Wild λ/2 shunt series	open/shorted stubs, λ/2 long section, requires ground connection coupled lines, λ/2 long section	Broadband to octave bandwidths, planar circuits	[12]
Low/High Impedance Section	transmission line section, λ/2 long very simple structure	Narrowband, planar circuits and waveguide	This study
Coupled Line Section	Coupled lines λ/4 long	Broadband, planar circuits	This study

Symmetric Coupler	Coupler, high complexity	Ultrawideband 1:10	[16]
Schiffman type network	Coupled lines λ/4 long Multisection, complex structure	Ultrawideband	[17]
LC-network	Lumped components	Low frequency, high volume	[8]
Variable Phase Shifter	Varactor, PIN-diodes, Metamaterials	Low frequency, high volume, tuneable	[7]
Grounded Shunt Stub	Distributed, Simple structure	Octave bandwidth, high frequency	[2]

Qualitative comparison of various differential phase shifters.

A. The high/low impedance λ/2 transmission line section

From [18], the ABCD parameters of an ideal transmission line, half a wavelength long at center frequency f_0, can be written as:

$$ABCD = \begin{bmatrix} \cos\theta & jZ_T\sin\theta \\ jY_T\sin\theta & \cos\theta \end{bmatrix} \tag{3}$$

$$\theta = \pi\frac{f}{f_0} \tag{4}$$

where Z_T and Y_T are the characteristic impedances and admittances, respectively, of the transmission line section. From the ABCD parameters, the S_{11} and S_{21} parameters are easily calculated by using standard transformation formulas; the input return loss, insertion loss and through phase can then be defined.

The relative through phase difference between a transmission line section, with a length θ, a normalized characteristic impedance z_T, and a matched transmission line of electrical length $K\theta$ (see Fig. 3), can be expressed as:

$$\Delta\varphi(\theta) = K\theta - \tan^{-1}\left\{\frac{z_T + y_T}{2}\tan\theta\right\} - \pi \tag{5}$$

$$\theta \in \left(\frac{\pi}{2}, \frac{3\pi}{2}\right)$$

with y_T being the normalized admittance and K a constant. It is shown that the normalized impedance and admittance terms contribute equally to the total phase difference. This means that, for any low impedance line section, there exists a high impedance line section that will produce the same through phase perturbation. Furthermore, imposing a matched condition for the filter section the minimum length is found

to be 180 degrees ($\theta_0 = \pi$) at centerfrequency. We then see that the phase difference for a $\lambda/2$ long section at centre frequency equals to:

$$\Delta\varphi(\theta_0) = (K-1)\pi \qquad (6)$$

which yields the value of K for a desired phase shift $\Delta\varphi_0$. One immediate conclusion is that it is not the impedance of the filter section, but rather the length of the matched reference line, that sets the nominal phase difference. Differentiating the phase function in (5) with respect to θ we get:

$$\Delta\varphi'(\theta) = K - \frac{z_T + y_T}{2} \frac{1 + \tan^2\theta}{1 + \left(\frac{z_T + y_T}{2}\right)^2 \tan^2\theta} \qquad (7)$$

By setting the derivative to zero, which is the condition for a local minimum and maximum, and then solving for θ, a direct expression of the phase ripple for a given K as a function of characteristic impedance Z_T can be derived.

$$\theta_{min,max} = \pi \pm \tan^{-1}\sqrt{\frac{\frac{(z_T + y_T)}{2} - K}{K\left(\frac{z_T + y_T}{2}\right)^2 - \frac{z_T + y_T}{2}}} \qquad (8)$$

As K is set by the required phase difference, it is the characteristic impedance that will define the ripple. We then see traditional trade off between bandwidth and maximum allowed phase deviation when varying Z_T. By studying the $\lambda/2$ filter group delay in (7), it is found that the value of K must be larger than one in order to have a constructive phase difference. In addition, a real solution of (8), which is the condition for ripple in the phase response on Z_T for a given K, leads to an upper constrain on K such that:

$$1 < K < \frac{z_T + y_T}{2} \qquad (9)$$

The results from numerical analysis of the phase deviation bandwidth and phase ripple vs. normalized characteristic impedance holding the phase difference as a parameter is plotted in Fig. 4 together with the simulated 10 dB input return loss bandwidth of the half wavelength filter.

B. The λ/4 open ended coupled line section

In this section we will study the single open-ended coupled line section for differential phase shifting (see Fig. 5). The theory of coupled transmission line structures was developed by Jones and Bolljahn in 1956 [19]. It was later generalised to include inhomogeneous dielectric mediums having unequal even-mode and odd-mode phase velocities by Zysman and Johnson in 1969 [20]; from this, the ABCD parameters of a quarter wavelength long (at centre frequency f_0) homogenous coupled line section with open ends are found to be:

$$ABCD = \begin{bmatrix} \dfrac{(Z_e + Z_o)}{(Z_e - Z_o)} \cos\theta & \dfrac{j}{2} \dfrac{(Z_e + Z_o)^2 \sin^2\theta - 4Z_e Z_o}{(Z_e - Z_o)\sin\theta} \\ \dfrac{2j\sin\theta}{(Z_e - Z_o)} & \dfrac{(Z_e + Z_o)}{(Z_e - Z_o)} \cos\theta \end{bmatrix}$$

(10)

$$\theta = \frac{\pi}{2} \frac{f}{f_0}$$

(11)

where Z_e and Z_o are the even and odd mode impedances of the coupled line section and the electrical length of the coupled lines is 90° at the centre frequency.

The expressions for S_{11} and S_{21} for the open ended coupled line section are readily calculated from the ABCD parameters using standard transformation formulas. The details of the mathematical steps are not accounted for here, however we conclude that, by studying the numerator in the expression for the S_{11} parameter, we find the following simple relation for a matched condition at the centre frequency for the characteristic system impedance.

$$Z_{0,C} = \frac{Z_e - Z_o}{2}$$

(12)

This condition however is used to simplify the analytical design. For optimum design implementations a slight mismatch is desirable, giving more flexibility, but also a more broadband response. The design could also benefit from using inhomogenous coupled lines, which is the case for microstrip circuits, as shown in [21]. Holding (12) true, the relative through phase difference between the open ended coupled line section of length θ, and a matched transmission line of electrical length $K\theta$, can be expressed as:

$$\Delta\varphi(\theta) = K\theta - \tan^{-1}\left\{\frac{(\rho^2+1)\sin^2\theta - 2\rho}{(\rho^2-1)\cos(\theta)\sin(\theta)}\right\}, \qquad \theta \leq \frac{\pi}{2} \tag{13}$$

with ρ being the even to odd mode impedance ratio. At centre frequency ($\theta_0 = \pi/2$) the phase difference equals to

$$\Delta\varphi_0 = \varphi(\theta_0) = \frac{\pi}{2}(K-1) \tag{14}$$

from which K can be found by inserting the required phase shift. By differentiating φ, with respect to θ and setting the expression equal to zero, the minimum and maximum points can be found numerically. The bandwidth and phase deviation versus coupling factor for different phase shifts are plotted in Fig. 6. The maximum coupling C for a coupled line section occurs when it is a quarter wavelength long and is defined as [22]:

$$C = \frac{\rho+1}{\rho-1} \tag{15}$$

C. Balanced and multisection λ/2 high/low impedance lines or λ/4 open ended coupled lines section designs

The performance and feasibility of differential phase shifters can be improved [14],[23]-[24], by using either a second dispersive network in the reference path, multiple sections, or a combination thereof, see Fig 1. In the case of the coupled line based differential phase shifter topology, a balanced design having coupled sections in both arms, leads to that a higher coupling factor can be used for realisation of lower phase shifts resulting in less tightly spaced lines.

In table 2, design parameters for different types of single section, balanced and multisection phase shifter topologies are presented with the corresponding phase imbalance and 10 dB input return loss bandwidth.

TABLE II
DESIGN PARAMETERS FOR VARIOUS DIFFERENTIAL PHASE SHIFTERS

			HIGH/LOW IMPEDANCE NETWORKS					
	φ_0	$Z_{1\alpha}$	$Z_{2\alpha}$	$Z_{3\alpha}$		K	R	$B\ (\%)$
1 section	90°	2.70	-	-		1.5	0.5°	20
2 section	90°	0.56	1.98	-		2.5	0.6°	30
3 section	90°	0.68	1.90	0.68		3.5	2°	40

					COUPLED LINE NETWORKS								
	φ_0	$Z_{e1,\alpha}$	$Z_{o1,\alpha}$	$Z_{e2,\alpha}$	$Z_{o2,\alpha}$	$Z_{e1,\beta}$	$Z_{o1,\beta}$	$Z_{e2,\beta}$	$Z_{o2,\beta}$	K	$\Delta\varphi$	$B\ (\%)$	C_{min} (dB)
1 section	45°	3.62	1.41	-	-	3.26	1.00	-	-	0.5	0.8°	54	5.5
1 section	90°	4.10	1.98	-	-	3.46	1.19	-	-	1	1°	40	6.2
2 section	180°	3.28	1	3.28	1	-	-	-	-	4	2°	50	5.5

Design parameters and performance characteristics for various phase shifter designs showing nominal phase difference φ_0, normalised impedances Z_x, K factor for reference line length, phase ripple R, relative bandwidth B and minimum coupling coefficient C_{min}. The minimum relative bandwidth is used looking at the 10 dB input return loss and the maximum phase ripple R as specified.

III.   DESIGN OF 45° AND 135° PHASE SHIFTER HYBRIDS

To split the signal into the differential phase shifter network, any 3 dB hybrid with reasonable output isolation can be used, given that the phase response of this component is taken into account. Without isolation, any reflection of significant magnitude, that causes a standing wave in between the two inputs of the phase shifter network, would spoil the phase balance of the phase shifter. We choose to use a Wilkinson divider [25]-[26], consisting of two even mode sections and one coupled odd mode section, having a simulated isolation better then 15 dB and input and output return loss better then 18 dB over the 9-15 GHz frequency range. In Fig. 7 a schematic of the phase shifter hybrid is shown.

Two differential phase shifters, based on the proposed circuit topologies, were designed and implemented in microstrip technology on a 20 mil thick Rogers RO4003 material, with a center frequency

of 12 GHz. Standard PCB manufacturing was used with approximately 50 μm thick copper lines with minimum feature sizes of approximately 100 μm and 25 μm tolerances.

The first differential phase shifter hybrid was based on the single half wavelength section filter and was designed for a 45° differential phase shift; this can be considered as an upper limit for this particular phase shifter topology, as a very low (or high) impedance Z_T leads to a narrow band insertion loss response. From (6), we find that K must equal to 1.25 giving a total reference line length of 225° at the center frequency. In Fig. 3 we see that an impedance of 22.5 Ω (alternatively 111.1 Ω) will result in a 1 degree phase deviation over a 20% relative bandwidth limited by the input return loss and not the phase response. However, with a 22.5 Ω line, it is difficult to realize why we had to settle with 25 Ω section that in theory should give no ripple by looking at (8).

The second differential phase shifter hybrid was a single quarter wavelength long open-ended coupled line section type and was designed for a 135° phase shift. From (14), K is calculated to 2.5, giving a total reference line length of 225°. From Fig. 5 we find the coupling factor for a 150° phase shift with 1° of phase deviation and 40% relative bandwidth to be approximately 8 dB. Using (15), the even to odd mode ratio, ρ, is calculated to 2.32; when inserted in (12) we are given a starting value for the even and odd mode impedances Z_e and Z_o equal to 176 Ω and 76 Ω, respectively. Further optimisation using a linear circuit simulator, leads to an even mode impedance of 160 Ω and a odd mode impedance of 66 Ω, giving a 40% relative phase bandwidth with less then 0.5° of phase deviation.

IV. SIMULATION AND MEASUREMENT RESULTS

Circuits were tested with an Agilent E8361A PNA, using a HP 85052B 3.5 mm calibration kit in a full 2-port coaxial calibration setup, with the third port terminated in a matched load, see Fig. 9 for circuit assembly and testfixture. Simulated results are based on 3D electromagnetic modeling using the CAD software HFSS from Ansoft; the main difference is that a completely shielded surrounding has been used in the models. The typical input return loss of the relatively rugged SMA connector was measured to 10 dB or better, back to back over the band however for the 45° hybrid one of the output ports had an input return loss peak at 13.5 GHz as bad as 5 dB. Measured and simulated results of the phase shifter hybrids phase and amplitude responses are presented in Fig. 10 and Fig. 11. In Fig. 12, the simulated and measured input

return loss is plotted including connectors and the Wilkinson power divider.

The discrepancies between measured and simulated results come in part from the mismatch in the coaxial to microstrip launch. The beating in the input return loss measurements has a periodicity of about 2.2 GHz, corresponding to a $\lambda/2$ distance in between the input and output connectors. The performance and repeatability of the coaxial microstrip launcher would, most likely, improve by switching to a smaller high performance SMA connector design. Time-domain techniques such as gating of through and reflect measurements could also be applied. Such measurements rely on high time resolution given by the bandwidth of the network analyzer and/or a large physical separation between device and connector.

The circuit manufacturing tolerances would also have an effect on the performance of the 135° phase shifter, which uses tightly spaced and relatively narrow coupled lines. The diverging phase difference comparing measured and simulated phase response for the 45° phase shifter in Fig.6 could be caused by reflections in the SMA-connector or leakage/radiation from the open microstrip environment. From an assembly tolerance perspective, a total displacement between the output connectors, in the order of 100 μm is reasonable to expect, corresponding to about 3° at 12 GHz. This error could be minimised if the output connectors of the test fixture were positioned at the same side of the PCB.

V. CONCLUSIONS

A theoretical analysis for the synthesis of two new types of differential phase shifters using basic high/low-impedance transmission line sections or coupled line sections has been presented and verified experimentally. The half wavelength high/low impedance section based phase shifter has a practical upper limit of total phase shift of about 45°; at this point the impedance level drops below 25 Ω or increases above 100 Ω and the 10 dB input return loss bandwidth is reduced to about 20%. Moving to multiple section designs a 90° phase shift can be achieved with increased bandwidth keeping the transmission line impedances within the 25 Ω to 100 Ω range. The inherently narrowband response for this device will be a limiting factor increasing the insertion loss; however, for some applications, it might still be an interesting alternative owing to its extreme simplicity.

The open-ended single coupled line section phase shifter can reach octave bandwidths for differential phase shifts ranging from 90° to 180° at coupling levels of 5.5 dB to 9 dB. Low coupling levels call for

high definition patterning techniques; such designs are better suited for MMIC and thinfilm applications or multilayer PCB technology using broadside couplers. A balanced topology is proposed using the coupled line filter in each of the differentials improving the feasibility of the design as the required coupling level is increased. Using multiple coupled line sections seems to give some additional improvement in the input return loss and sharpness of the filter response, but at the cost of a lower coupling factor. The compact format, wide span of realisable phase shifts and broad bandwidth, should make this topology an interesting alternative for applications requiring differential phase shifters.

VI. ACKNOWLEDGMENT

REFERENCES

[1] J. Butler and R. Lowe, "Beam-forming matrix simplifies design of electronically scanned antennas", *Electronic Design*, vol. 9, pp.170-173, April 1961.

[2] X. Tang and K. Mouthaan, "Phase-Shifter Design Using Phase-Slope Alignment With Grounded Shunt λ/4 Stubs", *IEEE Trans. Microw. Theory Tech.*, vol. 58, no. 6, pp. 1573-83, June 2010.

[3] S. Maas, "Nonlinear Microwave Circuits", Artech House, Inc., ISBN 0-7803-3403-5, pp. 209-230 1988.

[4] I.-H. Lin, K.M.K.H. Leong, C. Caloz and T. Itoh, "Dual-band sub-harmonic quadrature mixer using composite right/left-handed transmission lines", *IEEE Trans. Antennas Propagat.*, vol. 153, no 4, pp. 365-375, August 2006.

[5] P. Sobis, J. Stake and A. Emrich, "A 170 GHz 45° Hybrid for Submillimeter Wave Sideband Separating Subharmonic Mixers", *IEEE Microw. Wireless Compon. Lett.*, vol. 18, no. 10, pp. 680-682, October 2008.
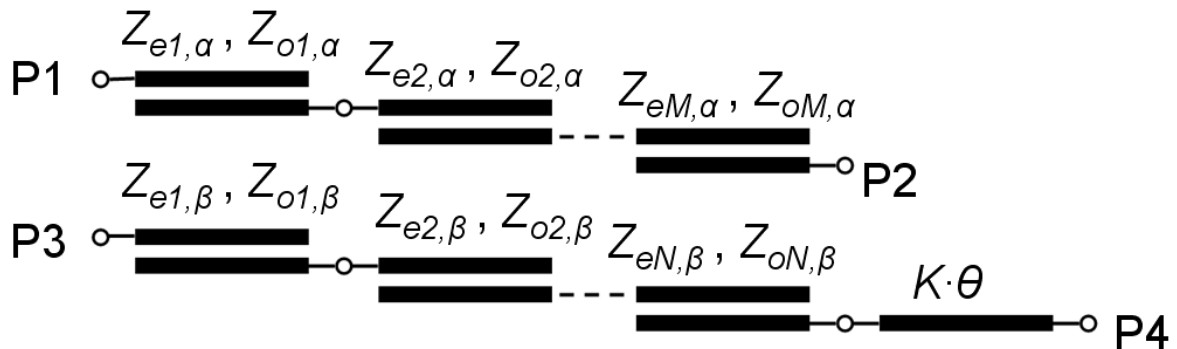
[6] B. Thomas, S. Rea, B. Moyna, B. Alderman and D. Matheson, "A 320-360 GHz Subharmonically Pumped Image Rejection Mixer Using Planar Schottky Diodes", *IEEE Microw. Wireless Compon. Lett.*, vol. 19, no. 2, pp. 101-103, February 2009.

[7] S. Koul and B. Bhat, Microwave and Millimeter Wave Phase Shifters. Norwell, MA: Artech House, 1991.

[8] D. Kuylenstierna and P. Linnér, "Design of broad-band lumped-element baluns with inherent impedance transformation", *IEEE Trans. Microw. Theory Tech.*, vol. 52, no. 12, pp. 2739-45, December 2004.

[9] J. Dittloff, F. Arndt and D. Grauerholz, "Optimum Design of Waveguide E-Plane Stub-Loaded Phase Shifters", *IEEE Trans. Microw. Theory Tech.*, vol. 36, no. 3, pp. 582-587, March 1988.

[10] B. M. Schiffman, "A new class of broad-band microwave 90-degree phase shifters", *IRE Trans. Microw. Theory Tech.*, vol. 6, no. 2, pp. 232-237, April 1958.

[11] J. L. R. Quirarte and P. J. Starski, "Synthesis of Schiffman Phase Shifters", *IEEE Trans. Microw. Theory Tech.*, vol. 39, no. 11, pp. 1885-1889, November 1991.

[12] R. B. Wilds, "Try λ/8 stubs for fast fixed phase shifts", *Microwaves & RF*, vol. 18, pp. 67-68, December 1979.

[13] S. Cohn, "Parallell-Coupled Transmission-Line-Resonator Filters", *IRE Trans. Microw. Theory Tech.*, vol. 6, no. 2, pp. 223-231, April 1958.

[14] J. L. R. Quirarte and P. J. Starski, "Novel Schiffman Phase Shifters", *IEEE Trans. Microw. Theory Tech.*, vol. 41, no. 1, pp. 9-14, January 1993.

[15] C. P. Tresselt, "Broad-band tapered-line phase shift networks", *IEEE Trans. Microw. Theory Tech.*, vol. 16, no.1, pp. 51-52, January 1968.

[16] F. V. Minnaar, J. C. Coetzee and J. Joubert, "A Novel Ultrawideband Microwave Differential Phase Shifter", *IEEE Trans. Microw. Theory Tech.*, vol. 45, no.8, pp. 1249-1252, January 1997.

[17] V. Petrovich, I. Metelnikova, V. Tupikin and G. Chumaevskaya, "A New Structure of Microwave Ultrawide-band Differential Phase Shifter", *IEEE Trans. Microw. Theory Tech.*, vol. 42, no.5, pp. 762-765, May 1994.

[18] David M. Pozar, "Microwave and RF Design of Wireless Systems", John Wiley & Sons, Inc., ISBN 0-471-32282-2, pp. 55, 2001.

[19] E. M. T. Jones and J. T. Bolljahn, "Coupled-strip-transmission line filters and directional couplers", *IRE Trans. Microw. Theory Tech.*, vol. 4, pp. 75-81, April 1956.

[20] G. I. Zysman and A. K. Johnson, "Coupled Transmission Line Networks in an Inhomogeneous Dielectric Medium", *IEEE Trans. Microw. Theory Tech.*, vol. 17, no. 10, pp.753-759, October 1969.

[21] J. Allen, "Inhomogenous Coupled-Line Filters with Large Mode-Velocity Ratios" , *IEEE Trans. Microw. Theory Tech.*, vol. MTT-22, no. 12, pp.1182-1186, December 1974.

[22] R. Collin, "Foundations for Microwave Engineering – Second Edition", McGraw Hill, ISBN 0-7803-6031-1, pp. 430-431 1992.

[23] B. Schiek and J. Kohler, "A Method for Broad-Band Matching of Microstrip Differential Phase Shifters", *IEEE Trans. Microw. Theory Tech.*, vol. 25, no. 8, pp. 666-671, August 1977.

[24] V. Meschanov, I. Metelnikova, V. Tupikin and G. Chumaevskaya "A New Structure of Microwave Ultrawide-Band Differential Phase Shifters", *IEEE Trans. Microw. Theory Tech.*, vol. 42, no. 5, pp. 762-765, May 1994.

[25] E. J. Wilkinson, "An n-way hybrid power divider" *IEEE Trans. Microw. Theory Tech.*, vol. 8, no.1, pp. 116-118, January 1960.

[26] S. B. Cohn, "A Class of Broadband three-Port TEM-Mode Hybrids" *IEEE Trans. Microw. Theory Tech.*, vol. 16, no. 2, pp. 110-116, February 1968.

High/Low Impedance-Network

$Z_{1\alpha}$ $Z_{2\alpha}$ $Z_{3\alpha}$ $Z_{4\alpha}$ $Z_{(M-1)\alpha}$ $Z_{M\alpha}$

P1   P2

$Z_{1\beta}$ $Z_{2\beta}$ $Z_{3\beta}$ $Z_{4\beta}$ $Z_{(M-1)\beta}$ $Z_{M\beta}$ $K\cdot\theta$

P3   P4

Coupled Line-Network

$Z_{e1,\alpha}$, $Z_{o1,\alpha}$ $Z_{e2,\alpha}$, $Z_{o2,\alpha}$ $Z_{eM,\alpha}$, $Z_{oM,\alpha}$

P1

P2

$Z_{e1,\beta}$, $Z_{o1,\beta}$ $Z_{e2,\beta}$, $Z_{o2,\beta}$ $Z_{eN,\beta}$, $Z_{oN,\beta}$ $K\cdot\theta$

P3

P4
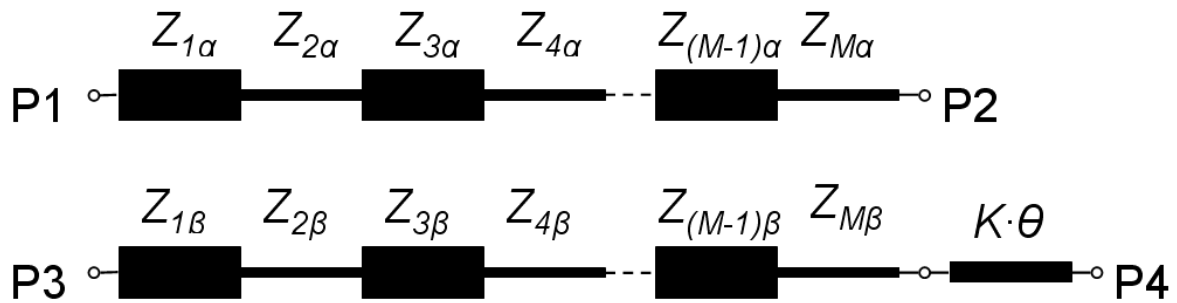
Fig.1. General balanced multiple section differential phase shifter using high and low impedance section or open-ended coupled line sections providing a constant relative phase difference comparing the S_{21} and S_{43} phase.
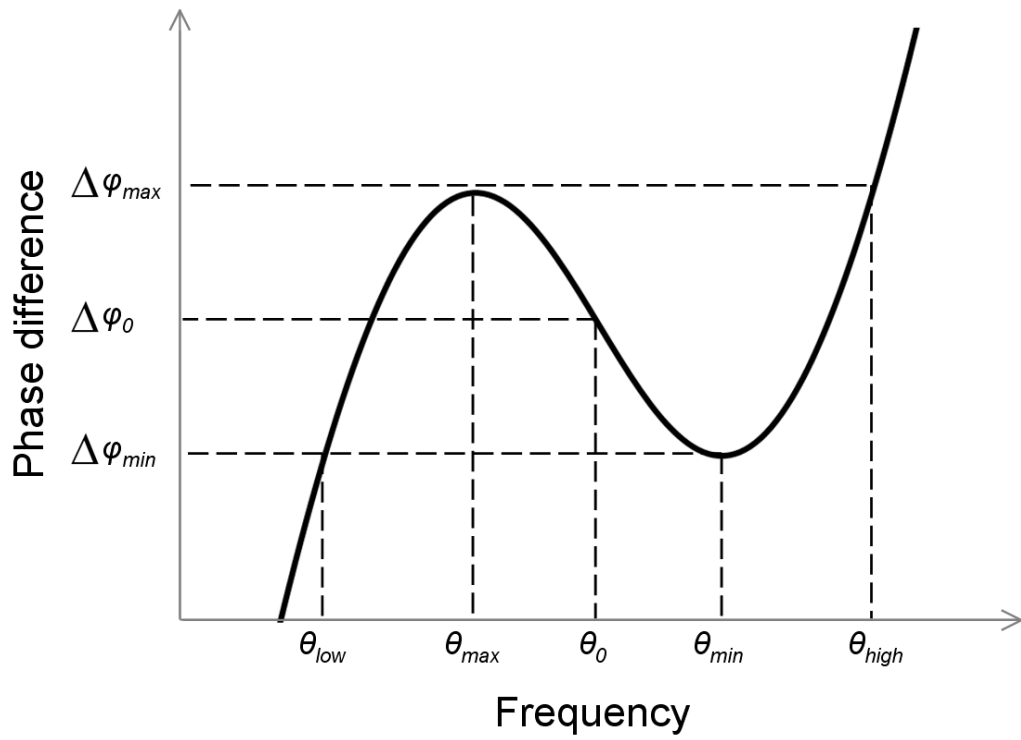
Fig.2. Typical phase response of a differential phase shifter.

High/Low Impedance-Network

$$Z_T , \theta$$

P1 ⊸ ▮ ⊸ P2

$$Z_C , K{\cdot}\theta$$

P3 ⊸ ▬ ⊸ P4
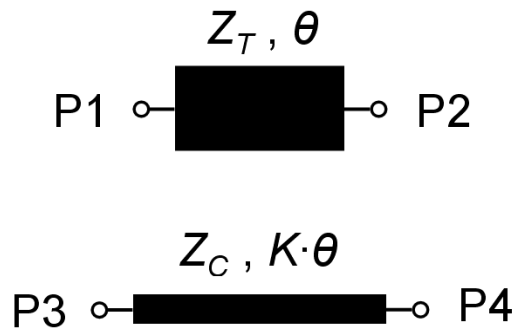
Fig.3. Differential phase shifter based on a single transmission line section with a characteristic line impedance Z_T different from Z_C.
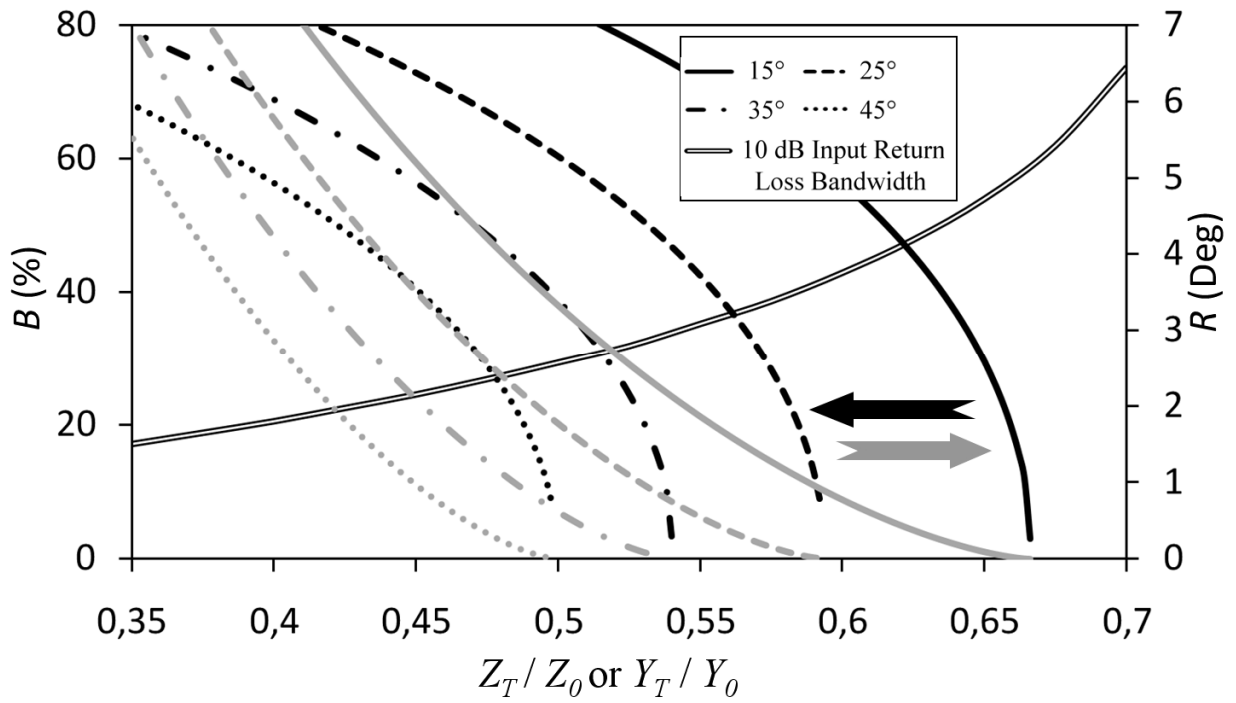
Fig.4. Theoretical phase ripple *R* and relative bandwidth of the phase response *B* for the half wavelength long section type differential phase shifter vs normalized characteristic impedance Z_T/Z_0 or normalized admittance Y_T/Y_0 plotted for different nominal phase shifts (15°, 25°, 35°and 45°). The simulated 10 dB Return Loss bandwidth is also plotted as it is an important limiting factor for this topology.

Coupled Line-Network

$$Z_e , Z_o , \theta$$

P1 ⊶▬▬▬

▬▬▬⊷ P2

$$Z_C , K{\cdot}\theta$$

P3 ⊶▬▬▬▬⊷ P4
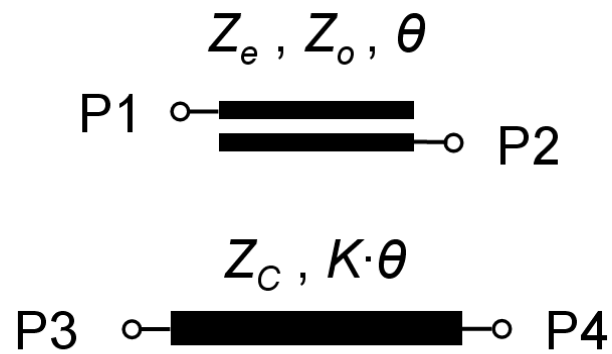
Fig.5. Differential phase shifter based on a single open-ended coupled line section with even and odd mode impedances Z_e and Z_o.
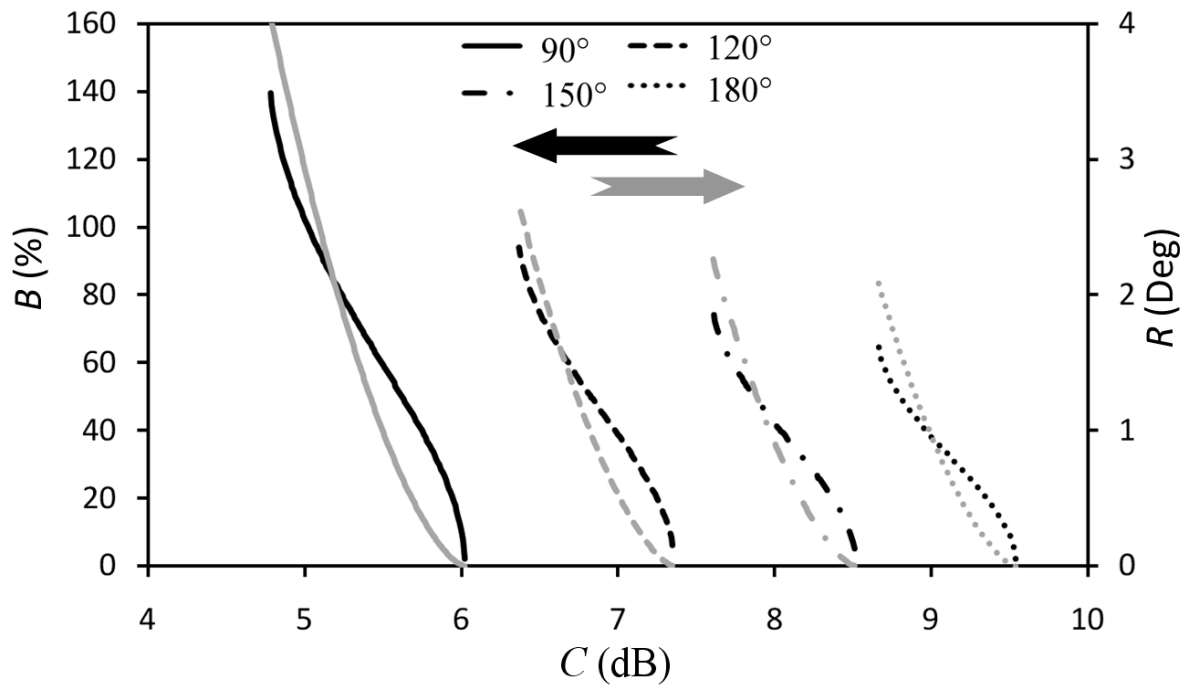
Fig.6. Theoretical phase ripple *R* and corresponding bandwidth of the phase response *B* for the quarter wavelength open ended coupled line section vs coupling coefficient *C* in dB at different nominal phase shifts (90°, 120°, 150°and 180°).
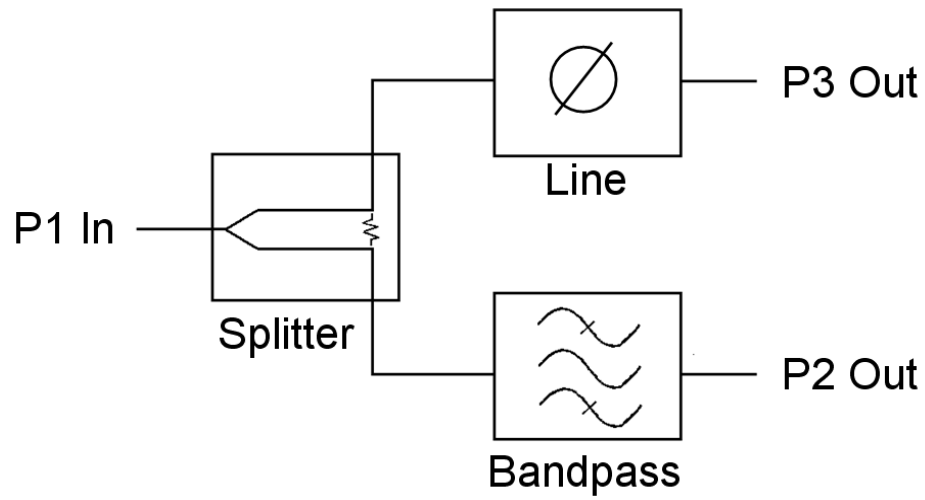
Fig.7. Schematic of a general two line differential phase shifter hybrid using a power divider with output isolation to split the signal to the differential phase shifter network.
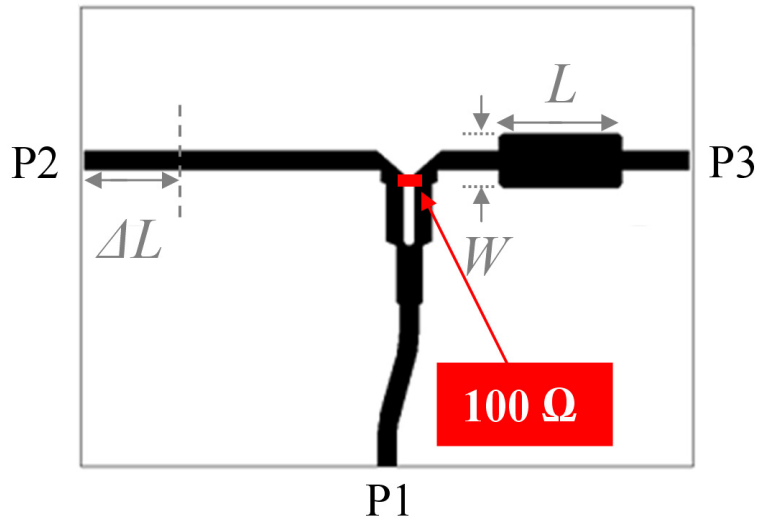
Fig.8. Layout of the 45° phase shifter hybrid using a Wilkinson divider loaded with a half wavelength long 25 Ω transmission-line section based differential phase shifter with W=3.00 mm, L=6.80 mm and offset length $\varDelta L$=2.48 mm.
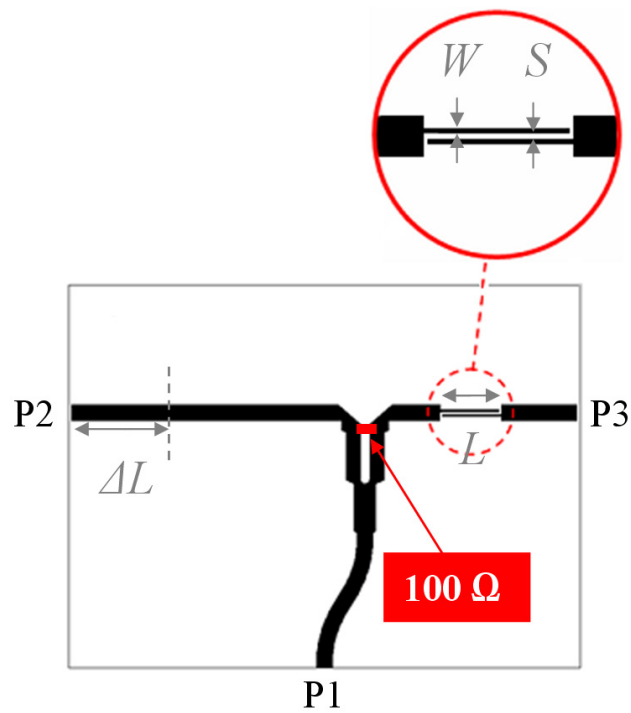
Fig.9. Layout of the 135° phase shifter hybrid using a Wilkinson divider loaded with a quarter wavelength long coupled-line section based differential phase shifter at the output with W=0.13 mm, L=4.05 mm, offset length ΔL=5.40 mm and the coupled line spacing S=0.15 mm.
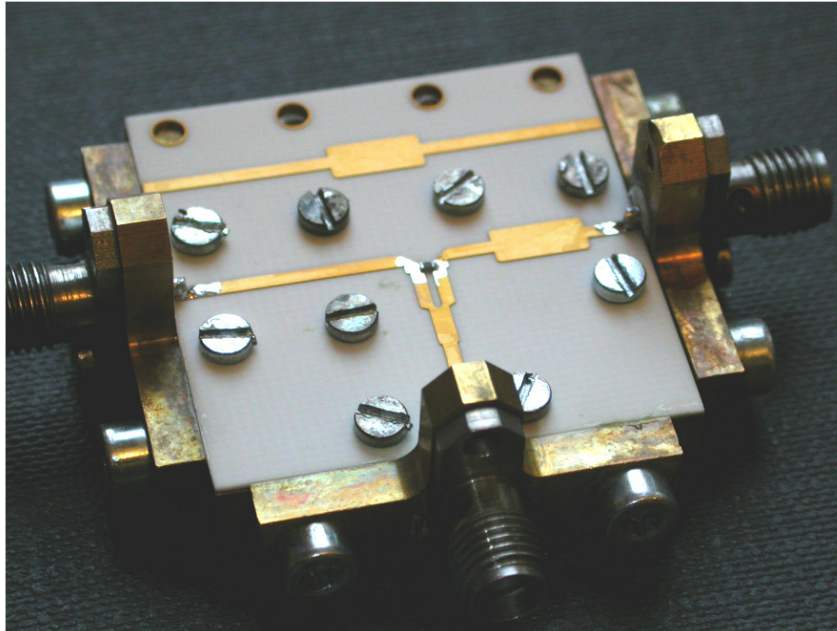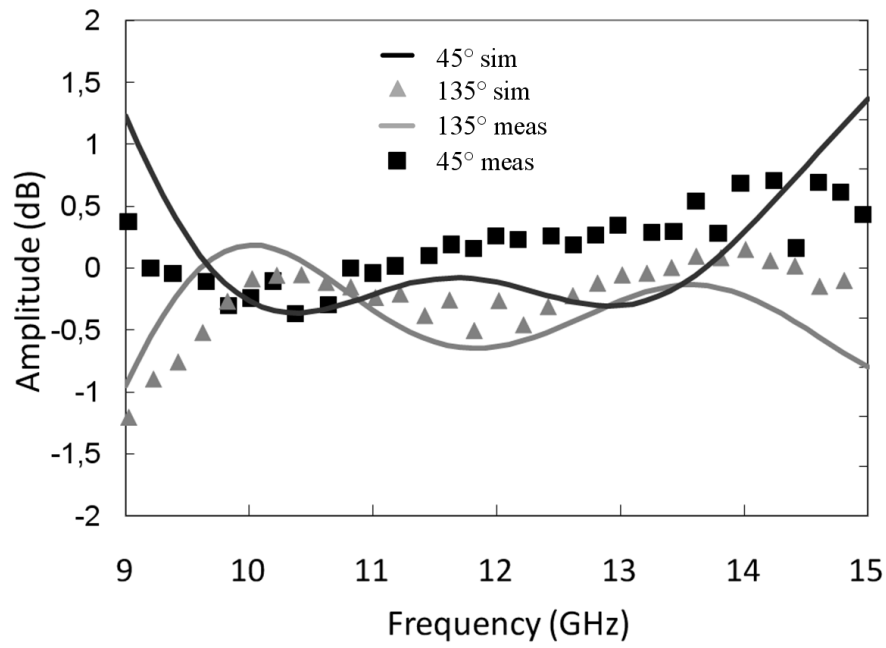
Fig.10. Photograph of the coaxial testfixture with a assembled phase shifter circuit. A 100 Ohm 0402-thinfilm resistor chip was soldered at the output of the Wilkinson power divider.
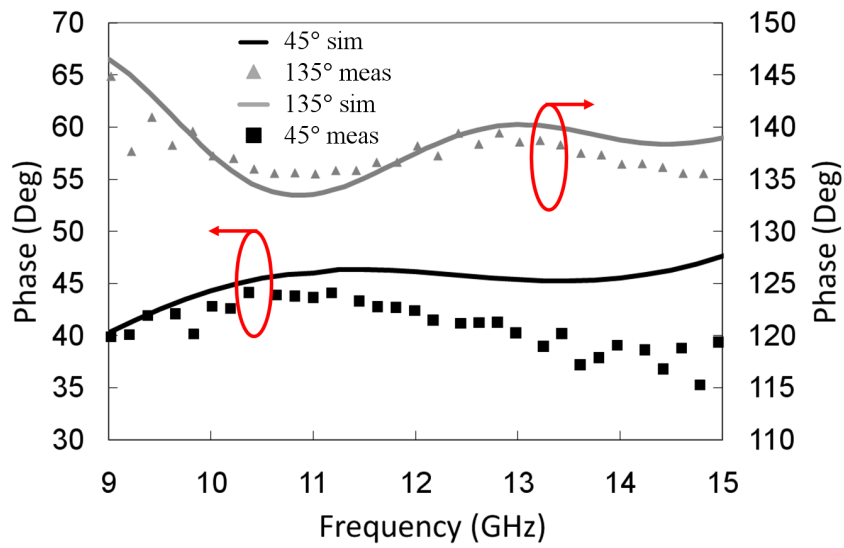
Fig.11. Simulated (line) and measured (dot) differential phase of the 45° (black) and 135° (grey) differential phase shifter circuits.

Fig.12. Simulated (line) and measured (dot) amplitude imbalance of the 45° (black) and 135° (grey) differential phase shifter circuits.
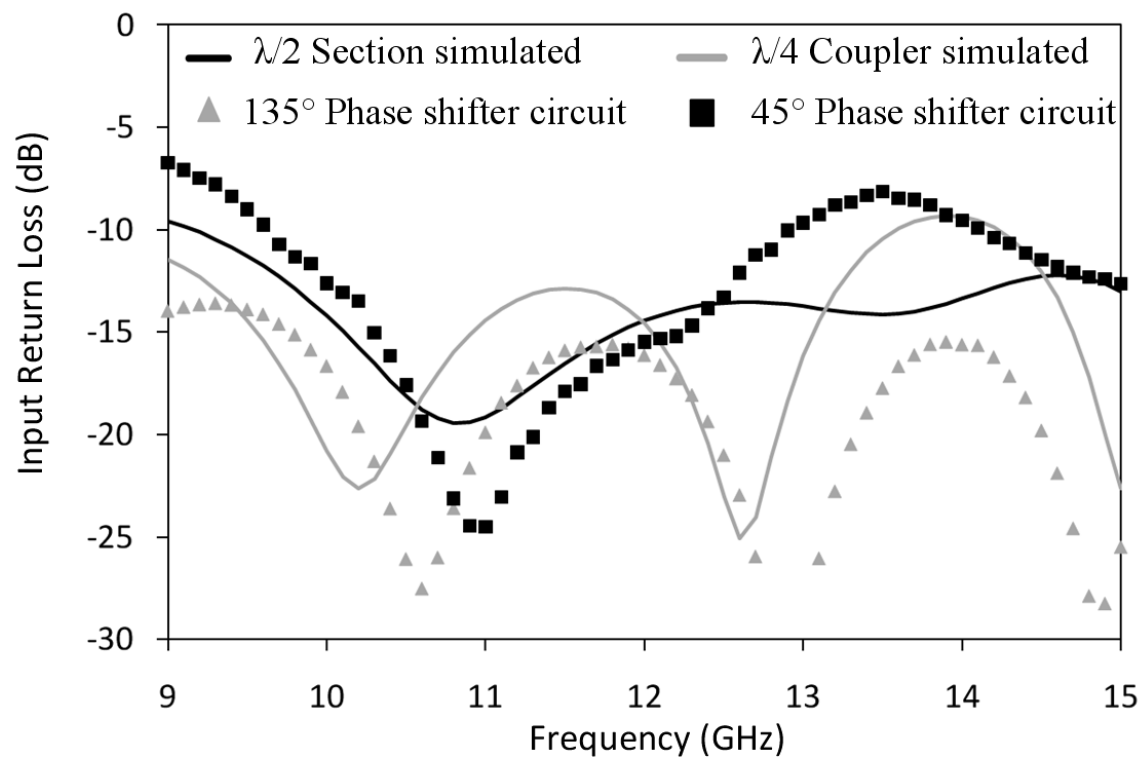
Fig.13. Simulated (solid) and measured (dot) input return loss of the differential phase shifter circuits.